

# Analysis of low frequency in offshore wind inner-array systems

I. Arrambide<sup>1</sup>

<sup>1</sup> Department of Electrical Engineering  
Escuela de Ingeniería de Guipúzcoa, University of the Basque Country  
Plaza Europa 1 – 20018 Donostia-San Sebastián (Spain)  
Phone number: +34 943 017214, e-mail: [inaki.arambide@ehu.eus](mailto:inaki.arambide@ehu.eus)

## Abstract.

Since large-scale offshore wind farms have been installed, generators have been constantly improving all the systems that make up these wind farms in order to obtain the cheapest energy price. Numerous improvements have been implemented to achieve this goal over the last few years, leading to a reduction in the levelised cost of energy (LCoE). In all projects using alternating current in both the collector system and the transmission system, the industrial frequency of 50/60 Hz has been used.

Recent studies have evaluated the possibility of using a lower frequency than 50/60 Hz, so that low frequency transmission not only increases the power capacity to be transmitted by cables, but also reduces cable losses. In this article, a detailed study of the energy losses in the collector system of a wind farm has been carried out as a function of frequency. The study shows a reduction in losses as the frequency is reduced, although the variation is not excessively large.

**Key words.** Offshore wind, LFAC, array system, transmission system, IEC 60287

## 1. Introduction

The construction of large-scale offshore wind farms (OWFs) is pushing developers to face new challenges related to the integration of the generated electricity into the existing onshore grid infrastructure. This requires the construction of new onshore substations or, as an alternative solution that is increasing interest, grid connection points that become vacant as nuclear or coal-fired generation plants are shut down.

Since the first OWFs were commissioned in the 1990s, different solutions for an efficient transmission grid have been applied. Due to electrical losses and load current, High Voltage Alternating Current (HVAC) technology is limited for long transmission systems or may even become unfeasible. Submarine cables in HVAC are mainly used to integrate offshore wind power due to the proximity to the coastline and this type of transmission will remain the majority option as long as it is feasible for each project, due to its maturity, price and simplicity. However, due to the development of long-distance and large-scale wind farms associated with the 2030 targets, HVAC technology will not be the most cost-effective solution in many cases,

so different transmission systems solutions are becoming the preferred solution.

Bearing all these issues in mind, this work is divided into following sections. Second section is focused on current transmission systems implemented in OWFs in operation. Third section shows the description of the problem related to Low Frequency-High Voltage Alternating Current (LF-HVAC). Fourth section analyses the power losses in the cables based on IEC 60287 and finally, some conclusions are stated together with a case study.

## 2. Analysis of transmission systems in OWFs

The different transmission systems applied for the integration of OWFs in operation around the world are as follows:

### A. Medium Voltage Alternating Current (MVAC)

Generally used for near-shore or intertidal projects, as well as small floating pilot projects without an offshore substation. The OWF's collector system is divided into several turbine strings that connect them to the onshore substation directly. Therefore, the voltage of the collector system is the same as that of the transmission lines typically in MVAC with a value range of 20~66 kV.

### B. High Voltage Alternating Current (HVAC)

This solution increases the voltage level of the transmission system to 110~220 kV and improves efficiency when power is transmitted to the onshore substation. It requires marine platform(s) along with additional electrical equipment as well as sizing of transformers, cables and all the remaining elements, which increases the final cost of the installation but the efficiency improvement compensates for it. Since submarine cables in HVAC present a capacitive effect, when the cables are very long, the charging and discharging currents produce a large amount of reactive power, which reduces the cable capacity and generates overvoltage problems.

As a result, some reactive power compensation is needed at both ends, even including an additional offshore reactive power compensation substation (RSC) at the

midpoint of the submarine cable system distance [1]-[3], which increases overall transmission costs.

In [4] the transmission capability depending on the frequency with compensation in both ends is shown, as can be observed in Figure 1.

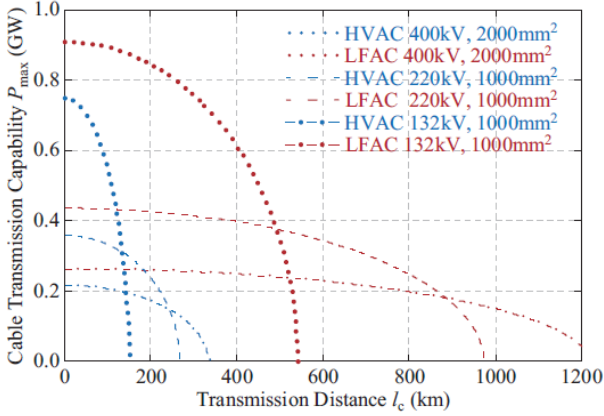


Fig. 1. Transmission capability vs frequency and distance.

### C. Combination HVAC & HVDC

Transmission of large amounts of power over long subsea transmission distances may not be an efficient option with HVAC, as it could result in an uneconomical solution or exceed the limits of technical feasibility. As offshore wind developers seek greater wind resources far from shore, HVDC technology has been chosen in some projects to integrate the generated power. In addition, VSC-HVDC technology is expected to play a key role in the development of the future plans included in the different National Energy and Climate Plans (NECPs), thanks to the advantages that overcome the limitations and drawbacks of HVAC lines and LCC-HVDC lines. The combination of HVAC links with VSC-HVDC comprises as basic elements an HVAC marine substation, HVAC transmission cables, two HVDC converter stations at both ends of the system and HVDC submarine cables linking the above converters in a point-to-point topology.

### D. High Voltage Direct Current (HVDC)

The wind farms currently being developed and planned to be built in this decade are applying the latest technological innovations related to HVDC transmission. On the one hand, OWFs have very high capacities so that their installed power covers the entire power capacity of the HVDC links. On the other hand, in recent years the voltage of the collector network connecting the turbines has been increased to 66 kV, which makes it possible to eliminate the HVAC substation and connect the collector system strings directly to the AC/DC converter, without the need for HVAC transmission. Thus, there is a reduction of the initial investment, increased efficiency and availability due to the reduction of electrical equipment required. This solution is already being implemented in the new transmission systems, although none of them are currently operational. On the other hand, it is also planned to implement higher voltages for more efficient transmission with lower losses called Direkt Konzept, with typical

values of  $\pm 525$  kV and 2 GW per link [5], under 2 GW Program initiative led by TenneT Dutch-German TSO.

In Figure 2, all projects developed in Europe have been summarised.

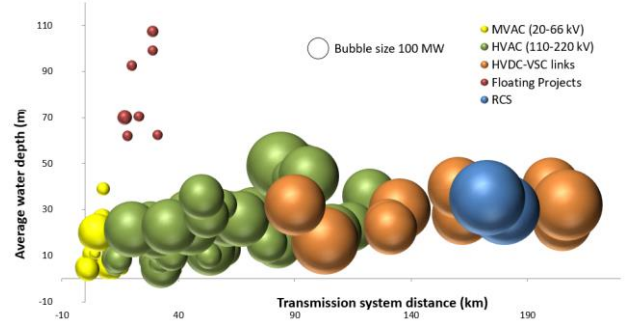


Fig. 2. Transmission systems in OWFs in Europe. Own elaboration.

## 3. Analysis of LF-HVAC

All transmission solutions explained above using HVAC technology have been implemented with industrial frequency of 50/60 Hz. To increase the capacity of HVAC lines, several authors [6]-[10] suggest a low frequency solution LF-HVAC, however, so far there is no commissioned offshore wind project using this option.

As an example deserve to be mentioned that a pilot project is being developed at 20 Hz in Yuhuan city, Taizhou prefecture, Zhejiang province in China. This experimental OWF is being developed by Huaneng Group and comprises 19 offshore wind turbines (OWTs) W16000/252 Shanghai Electric model, totalling 304 MW [11].

Nowdays the OWTs have a variable speed control thanks to a back-to-back converter inside the nacelle. It's main role of this double converter is to adapt the energy generation depending on the wind intensity to the grid frequency. So the grid side converter is the responsible to fix the output frequency.

## 4. Influence and analysis of LFAC in cables

### A. Overall losses

The total power losses in three-phase cables per meter are calculated from the general equation extracted from IEC 60287 as well as all corresponding formulas [12], as follows:

$$P_{\text{losses}}(\text{W/m}) = 3I^2 R_{\text{conductor,ac}}(1 + \lambda_1 + \lambda_2) + W_d \quad (1)$$

Where:  $I$  is the current flowing in the conductor (A),  $R_{\text{conductor,ac}}$  is the AC resistance of conductor ( $\Omega$ ),  $\lambda_1$  is the sheath loss factor,  $\lambda_2$  is the armour loss factor and  $W_d$  are the dielectric losses (W/m).

Since the cables are composed of three metal components, rather, conductor sheath and armour, three different losses

will be examined, which will depend on the current square. The dielectric losses represent the forth losses of the cable and will be calculated on the square of the voltage. The internal composition of the cables used for OWFs in collector systems is shown in Figure 3.

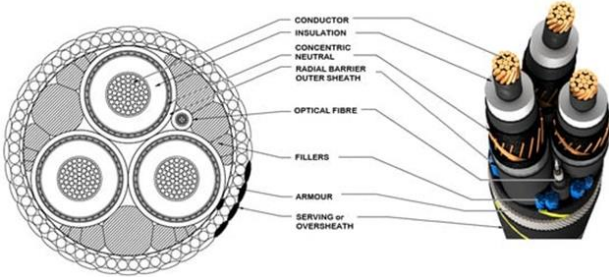


Fig. 3. Illustration of cross section and picture of typical MVAC cable in OWFs collector systems [13].

### B. Determination of conductor losses

Following the equation (1), the core losses typically made of cooper or aluminium row material can be expressed as:

$$P_{\text{conductor losses}} (\text{W/m}) = 3I^2 R_{\text{conductor,ac}}$$

The components in Equation (1) are calculated as follows:

$$I(A) = \sqrt{(L_{\text{conductor}} I_{\text{charge}})^2 + \left(\frac{P_{\text{turbine}}}{\sqrt{3} U_{\text{collector}} PF}\right)^2} \quad (2)$$

Where:  $L_{\text{conductor}}$  is the conductor length (m),  $I_{\text{charge}}$  represents the charge current (A/m),  $P_{\text{turbine}}$  is the power of offshore wind turbine (W),  $U_{\text{collector}}$  is the collector line-to-line RMS voltage (V) and  $PF$  means the power factor.

Additionally charge current has the following expression:

$$I_{\text{charge}} (\text{A/m}) = 2\pi f C U_{\text{collector}} / \sqrt{3} \quad (3)$$

Where:  $f$  is the frequency (Hz) and  $C$  represents the capacitance of the cable per meter (F/m).

As the main conclusion from the Equation 3, the  $I_{\text{charge}}$  is proportional to the frequency, so the lower the frequency the lower the current flowing in the conductor, making down the power losses. It should be noted that charge current is quite smaller than high power turbine's current so the total current flowing through conductor will not suffer appreciate changes if frequency changes.

From the point of view of the conductor's resistance, the formulas from IEC 60287 can be extracted taking into account that the maximum tolerable operational temperature is 90°C for cross-linked polyethylene (XLPE) insulation cables, according to data provided by cable manufacturers:

$$R_{\text{conductor,AC}}^{90} (\Omega/\text{m}) = R_{\text{conductor,DC}}^{90} (1 + y_s + y_p) \quad (4)$$

Where:  $y_s$  is the skin effect factor,  $y_p$  is the proximity effect factor and  $R_{\text{conductor,DC}}^{90}$  is the conductor's resistance at 90°C in DC ( $\Omega/\text{m}$ ). The former being:

$$R_{\text{conductor,DC}}^{90} (\Omega/\text{m}) = R_{\text{conductor,DC}}^{20} (1 + \alpha_m 70) \quad (5)$$

Where:  $R_{\text{conductor,DC}}^{90}$  is the conductor's resistance at 90°C in DC ( $\Omega/\text{m}$ ) data supplied by cable manufacturers in their catalogue, while  $\alpha_m$  is the conductor material's coefficient of resistance variation with temperature.

In the same way, the skin and proximity effect factors can be summarised as follows:

$$y_s = \frac{X_s^4}{192 + 0,8X_s^4} \quad (6)$$

$$X_s^2 = \frac{8\pi f K_s 10^{-7}}{R_{\text{conductor,DC}}^{90}} \quad (7)$$

$$y_p = \frac{X_p^4}{192 + 0,8X_p^4} \left( \frac{d_c}{s} \right)^2 \left[ 0,312 \left( \frac{d_c}{s} \right)^2 + \frac{1,18}{\frac{X_p^4}{192 + 0,8X_p^4} + 0,27} \right] \quad (8)$$

$$X_p^2 = \frac{8\pi f K_p 10^{-7}}{R_{\text{conductor,DC}}^{90}} \quad (9)$$

As well as the Equation (3) the conclusion about the reduction of frequency and the influence on the final value of conductor resistance is clear. Both skin and proximity effect factors will be slightly reduced because of reduction of frequency.

The final conclusion in relation to the conductor's losses in a 3-core submarine cable can be easily achieved. According to this section formulation, both magnitudes from the Equation 1 decrease if lower frequency comes from inverter grid side from the OWT. Even more, the relationship of frequency with these magnitudes is not linear, therefore the associated losses will not reflect a linear variation.

### C. Sheath losses

The sheath losses, as well as sheath loss factor  $\lambda_1$ , are calculated in IEC 60287 and the calculation for a 3-core type cable is as follows:

$$P_{\text{screen losses}} (\text{W/m}) = 3I^2 R_{\text{conductor,ac}} (\lambda_1) \quad (10)$$

Where:

$$\lambda_1 = \frac{3,2w^2}{R_{\text{conductor,AC}}^{90} R_{\text{screen}}^{90}} \left( \frac{2c}{d} \right)^2 10^{-14} \left[ 1 + \left( \frac{d}{d_a} \right)^2 \left( \frac{1}{1 + \frac{d_a}{300\delta}} \right) \right]^2 \quad (11)$$

Where:  $w$  is the angular frequency,  $R_{\text{screen}}^{90}$  is the screen's resistance at 90°C ( $\Omega/\text{m}$ ),  $c$  is the distance between the axis of a conductor and the centre of the cable (mm),  $d$  is the average diameter of the screen,  $d_a$  is the armour's average diameter (mm) and  $\delta$  is the equivalent width of the armature (mm).

#### D. Armour losses

The armour losses, as well as armour loss factor  $\lambda_2$ , are calculated in IEC 60287 and the calculation for a 3-core type cable is as follows:

$$P_{\text{armour losses}} (\text{W/m}) = 3I^2 R_{\text{conductor,ac}} (\lambda_2) \quad (12)$$

Where:

$$\lambda_2 = \frac{1,23 R_{\text{armour}}^{90}}{R_{\text{conductor,AC}}^{90}} \left( \frac{2c}{d_a} \right)^2 \frac{1}{1 + \left( \frac{2,7710^6 R_{\text{armour}}^{90}}{w} \right)^2} \quad (13)$$

Where:  $R_{\text{armour}}^{90}$  is the armour's resistance at 90°C ( $\Omega/\text{m}$ ).

#### E. Dielectric losses

$$P_{\text{dielectric losses}} (\text{W/m}) = W_d = 2\pi f C U_0^2 \tan \delta \quad (14)$$

Where:  $f$  is the frequency (Hz),  $C$  is the capacitance of the cable (F/m),  $U_0$  is the line-to-ground voltage (V) and  $\tan \delta$  is the insulation loss factor at frequency and operating temperature.

Since the cables used in collector systems are submarine ones, they are insulated and dielectric losses will occur [14]. Due to their insulation, three phenomena occur that cause three types of losses: (1) friction due to the oscillation of charges in the atoms of the insulation because of the alternating field, (2) a leakage current between core-screen-armour that causes additional losses, and (3) due to capacitor behaviour of the cable there will be a charge current across all longitude of the cable which acts generating reactive power.

### 5. Case study

In this case study the following assumptions have been made:

The OWT model chosen for this study is the generic 15 MW output power and 236 m of rotor diameter. The proposed case study for calculations, is based on the Weibull parameters  $c=10 \text{ m/s}$  and  $k=2.1$  for a mean wind speed of  $8,85 \text{ m/s}$  correspond for 150 m hub height.

For estimating energy annual production (AEP), an open source library named FLOW Redirection and Induction in Steady-state (FLORIS) developed by NREL is used [15]. This tool optimizes the AEP together with wake effect losses aiming to design the best solution of OWF turbines layout. It presents a control oriented model that predicts the characteristic of the wakes in a wind power farm as a function of the position of turbines and angle of the rotor.

Applying methodology described in [16] for optimizing collector array the OWF's layout will be made up of 12 strings with 5 OWT each linked by  $2 \times 630 \text{ mm}^2$  and  $3 \times 300 \text{ mm}^2$  of cooper cable.

Table I.-Conditions applied for cables

|   |
|---|
| Maximum temperature at continuous load: 90°C        |
| 3-core copper XLPE insulated 24/60 (72.5) kV cables |
| Frequency: 50 Hz                                    |
| Ambient temperature: 15°C                           |
| Burial depth of cables: 1 m                         |
| Thermal resistivity of surroundings: 1.0 K.m/W      |
| $K_s$ and $K_p$ coefficients: 1                     |

Table II.-OWF location conditions and design parameters

|  |   |
|--|---|
| Capacity:                                  | 1.2 GW                                  |
| Sea depth:                                 | 25 m                                    |
| Seabed temperature:                        | 15°C                                    |
| Cable burial:                              | 1.5 m                                   |
| Distance turbines prevailing direction:    | 10 D                                    |
| Distance turbines no prevailing direction: | 8 D                                     |
| Power factor:                              | 0,95                                    |
| Topology:                                  | Radial                                  |
| Inter-array voltage:                       | 66 kV                                   |
| Cable cross section:                       | 95 mm <sup>2</sup> -800 mm <sup>2</sup> |

Table III. – Technical values of cables at full power Vs frequency according to Equation (1)

| Frequency (Hz)                         | $I_{\text{charge}}$ (mA/m) |        | $R_{\text{conductor,ac}} (90^\circ\text{C})$ (m $\Omega/\text{m}$ ) |        | $\lambda_1$ |        | $\lambda_2$ |        |
|--|----------------------------|--------|---|--------|-------------|--------|-------------|--------|
| Cable cross section (mm <sup>2</sup> ) | 630                        | 300    | 630   | 300    | 630         | 300    | 630         | 300    |
| 60                                     | 4,5968                     | 3,4470 | 0,0635  | 0,1290 | 0,1827      | 0,0562 | 0,2356      | 0,0849 |
| 55                                     | 4,2138                     | 3,1603 | 0,0630  | 0,1288 | 0,1549      | 0,0473 | 0,2030      | 0,0721 |
| 50                                     | 3,8307                     | 2,8730 | 0,0624  | 0,1286 | 0,1291      | 0,0391 | 0,1717      | 0,0601 |
| 45                                     | 3,4476                     | 2,5857 | 0,0619  | 0,1284 | 0,1054      | 0,0317 | 0,1421      | 0,0491 |
| 40                                     | 3,0645                     | 2,2984 | 0,0615  | 0,1282 | 0,0838      | 0,0251 | 0,1145      | 0,0391 |
| 35                                     | 2,6815                     | 2,0111 | 0,0611  | 0,1280 | 0,0646      | 0,0192 | 0,0892      | 0,0302 |
| 33,3                                   | 2,5512                     | 1,9134 | 0,0610  | 0,1279 | 0,0586      | 0,0174 | 0,0812      | 0,0274 |
| 30                                     | 2,2984                     | 1,7238 | 0,0608  | 0,1279 | 0,0477      | 0,0141 | 0,0665      | 0,0223 |
| 25                                     | 1,9153                     | 1,4365 | 0,0605  | 0,1277 | 0,0333      | 0,0098 | 0,0468      | 0,0155 |
| 20                                     | 1,5322                     | 1,1492 | 0,0602  | 0,1276 | 0,0214      | 0,0063 | 0,0303      | 0,0100 |
| 16,7                                   | 1,2794                     | 0,9596 | 0,0601  | 0,1276 | 0,0149      | 0,0044 | 0,0212      | 0,0070 |



Table II. – Results of the study of different losses in whole collector system of the OWF Vs frequency

| Frequency (Hz) | Core losses (GWh) | Screen losses (GWh) | Armour losses (GWh) | Dielectric losses (GWh) | AED (GWh) |
|----------------|-------------------|---------------------|---------------------|-------------------------|-----------|
| 60             | 42,878            | 5,754               | 8,258               | 3,647                   | 4421,79   |
| 55             | 42,472            | 4,821               | 7,076               | 3,360                   | 4424,60   |
| 50             | 42,093            | 3,986               | 5,975               | 3,074                   | 4427,21   |
| 45             | 41,742            | 3,244               | 4,958               | 2,789                   | 4429,60   |
| 40             | 41,422            | 2,593               | 4,033               | 2,505                   | 4431,78   |
| 35             | 41,135            | 2,028               | 3,204               | 2,222                   | 4433,74   |
| 33,3 (50.2/3)  | 40,973            | 1,712               | 2,720               | 2,035                   | 4434,89   |
| 30             | 40,882            | 1,546               | 2,476               | 1,941                   | 4435,49   |
| 25             | 40,667            | 1,143               | 1,853               | 1,661                   | 4437,01   |
| 20             | 40,491            | 0,818               | 1,338               | 1,381                   | 4438,30   |
| 16,7 (50.1/3)  | 40,397            | 0,644               | 1,059               | 1,197                   | 4439,04   |

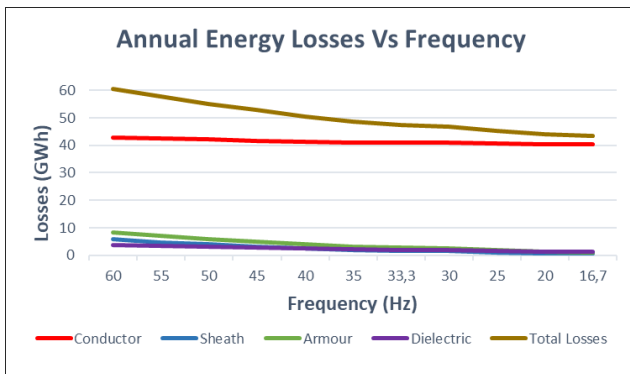


Fig. 4. Results of different losses vs frequency.

## 6. Conclusions

As results show in Table I and Table II, it is clear that technical values of the cables change with respect to frequency. The Equation 1 shows the parameters which establish the overall losses and all of them change if frequency changes. The lower the frequency the lower the values so it is obvious that lower frequencies will make the losses down. As dielectric losses depend directly on the frequency applied, it is clear that dielectric losses will be lower as well.

As Figure 4 shows, the losses related with frequency are slightly smaller as it decreases. Taking into account that an OWF's lifecycle could be large enough at the range about 30~40 years for next future plants, it seems reasonable to make an accurate assessment about the possibility of implementing LFAC in OWFs array systems, even more if transmission system takes the same technical solution.

## References

- [1] A. Tajer, M. S. Zouraraki, T. Kvarts, R. Østerø, T. Page, J. Hjerrild, "Hornsea projects 1 and 2 - Design and Optimisation of the Cables for the World Largest Offshore Wind Farms", 2019.
- [2] M. Lehmann, M. Pieschel, M. Juamparez, K. Kabel, L. H. Kocewiak, S. Sahukari, "Active Filtering in a Large-Scale STATCOM for the Integration of Offshore Wind Power", 2018.
- [3] J. Dakic, M. Cheah-Mane, O. Gomis-Bellmunt, E. Prieto-Araujo, "HVAC Transmission System for Offshore

Wind Power Plants Including Mid-Cable Reactive Power Compensation: Optimal Design and Comparison to VSC-HVDC Transmission", *IEEE Transactions on Power Delivery*, Vol. 36, No. 5, pp. 2814-2824, 2021.

- [4] X. Xiang, S. Fan, Y. Gu, W. Ming, J. Wu, W. Li, X. He, T. C. Green, "Comparison of Cost-effective Distances for LFAC with HVAC and HVDC in Their Connections for Offshore and Remote Onshore Wind Energy", *CSEE Journal of Power and Energy Systems*, Vol. 7, No. 5, pp. 954-974, 2021.

- [5] "Direkt Konzept. Schema Offshore Anbindung 2 GW" TenneT, June, 2022. <https://www.tennet.eu/about-tennet/innovations/2gw-program>

- [6] M. Carrasco, F. Mancilla-David, G. Venkataramanan, J. Reed, "Low frequency HVac transmission to increase power transfer capacity", *IEEE PES T&D Conference and Exposition*, pp. 1-5, 2014.

- [7] S. Chaithanya, N. B. Reddy, R. Kiranmayi, "A state of art review on offshore wind power transmission using low frequency AC system", *International Journal of Renewable Energy Research*, Vol. 8, pp. 141-149, 2018.

- [8] Y. Meng, S. Yan, K. Wu, L. Ning, X. Li, X. Wang, X. Wang, "Comparative economic analysis of low frequency AC transmission system for the integration of large offshore wind farms", *Renewable Energy*, Vol. 179, pp. 1955-1968, 2021.

- [9] J. Ruddy, R. Meere, T. O. Donnell, "Low Frequency AC transmission for offshore wind power: A review", *Renewable and Sustainable Energy Reviews*, Vol. 56, pp. 75-86, 2016.

- [10] S. Shneen, M. Abdul Hussein, J. Kadhum, S. Ali, "Application of LFAC 16 2/3Hz for electrical power transmission system: a comparative simulation study" *Telecommunication Computing Electronics and Control*, Vol. 17, pp. 1055, 2019.

- [11] "Single unit 16&18MW! Construction of offshore booster station of Huaneng Yuhuan No. 2 offshore wind power project started". Press release (In chinese).

- [12] IEC 60287 Calculation of the current rating - Part 1:

- Current rating equations (100 % load factor) and calculations of losses.

- [13] L. Resner, S. Paszkiewicz, "Radial Water Barrier in Submarine Cables, Current Solutions and Innovative Development Directions", *Energies*, Vol. 14, No. 10, 2021.

[14] L. Recio. “Pérdidas en el dieléctrico de los cables aislados. La tangente de delta” July, 2021. Prysmian Group. <https://www.prysmianclub.es/perdidas-en-el-dielectrico-de-los-cables-aislados-la-tangente-de-delta/> (In Spanish)

[15] “FLOw Redirection and Induction in Steady state” (FLORIS). <https://www.nrel.gov/wind/floris.html>

[16] I. Arrambide, I. Zubia, A. Madariaga. “Re-optimizing array cable systems in offshore wind farms using 66 kV voltage”, Renewable Energy & Power Quality Journal (RE&PQJ) ISSN 2172-038 X, No.18 June 2020.